A study of the x-irradiated $Cs_5H_3(SO_4)_4 \cdot H_2O$ crystal by EPR in the 80 - 415 K temperature range

1997 J. Phys.: Condens. Matter 9 4813

(http://iopscience.iop.org/0953-8984/9/23/005)

J. Phys.: Condens. Matter **9** (1997) 4813–4821. Printed in the UK PII: S0953-8984(97)79394-9

A study of the x-irradiated $Cs_5H_3(SO_4)_4 \cdot H_2O$ crystal by EPR in the 80–415 K temperature range

S Waplak†, W Bednarski†, A I Baranov‡ and L A Shuvalov‡

† Institute of Molecular Physics, Polish Academy of Sciences, Smoluchowskiego 17/19, 60-179 Poznań, Poland

‡ Institute of Crystallography, Russian Academy of Sciences, Leninsky prospect 59, 117333 Moscow, Russia

Received 8 November 1996

Abstract. The EPR spectra of the x-irradiated fast proton conductor $Cs_5H_3(SO_4)_4 \cdot H_2O$ were investigated in the temperature range of 80–415 K.

Two kinds of paramagnetic SO_4^- centres with different proton configurations below about 370 K and freeze-out behaviour of one of them below about 200 K were observed. The role of acid proton dynamics with respect to the glassy-like transition is discussed.

1. Introduction

$Cs_5H_3(SO_4)_4 \cdot H_2O$—abbreviated as PCTHS—belongs to a new family of superionic conductors [1] which exhibits dynamic disordering of the H-bond network in the high-temperature state. This kind of proton disorder means proton disorder in the double-well potential of the H-bonds as well as disorder of the H-bonds themselves [2, 3]. The peculiarity of this compound is the suppression of the phase transition into the ordered ferroelectric phase.

Instead PCTHS was found to be the first in the family to transform into a glasslike state on cooling below $T_g = 260$ K. In contrast to the well known family of mixed hydrogen bonded crystals such as KDP/ADP [4] the glasslike freezing in PCTHS does not need a competition interaction. This is the reason why this problem is very interesting in solid state physics.

At room temperature PCTHS belongs [3] to the space group $P6_3/mmc$ (D_{6h}). The crystal structure comprises two types of SO_4^{2-} tetrahedron which form alternating networks in the (001) layers: 'static' $SO_4^{2-}(1)$ and 'mobile' $SO_4^{2-}(2)$ ones. The latter appear to be dynamically disordered: their centres of gravity (i.e. S atoms) remain static and the vortices perform reorientations among three different positions. Adjacent $SO_4^{2-}(1)$ and $SO_4^{2-}(2)$ tetrahedra are partially connected by proton O–H...O bonds. The positions of these bonds depend on instantaneous orientations of $SO_4^{2-}(2)$ tetrahedra.

In the crystal structure of PCTHS three types of hydrogen bond exist. Their centres occupy 6(h), 12(k) and 24(l) sites with the lengths 2.68, 3.03 and 2.89 Å respectively and occupancy rates are $\frac{1}{3}$, $\frac{1}{6}$ and $\frac{1}{12}$.

The double disorder of protons (intra-bond and inter-bond) favours both proton transport at high temperatures and the proton-glassy state at low temperatures.

0953-8984/97/234813+09$19.50

We perform EPR studies of x-irradiated PCTHS with the aim of looking closely (from a local probe point of view) at glassy-freezing phenomena.

The X-irradiation can produce in $Cs_5H_3(SO_4)_4 \cdot H_2O$ samples the SO_4^- paramagnetic centres. After x-irradiation the breaking of hydrogen bonds (preferably the longest one) can also lead to EPR superhyperfine proton structure due to electron spin and nuclear proton spin interaction.

2. Experimental details

The $Cs_5H_3(SO_4)_4 \cdot H_2O$ crystals were grown by slow evaporation of an aqueous solution at room temperature [1].

Colourless, transparent, single crystals of PCTHS were next x-irradiated (tungsten cathode, 40 kV, 10 mA) for 5–6 h. The sample after x-irradiation remained colourless.

The EPR measurements were made with an X-band spectrometer operating with a liquid-nitrogen system of temperature control and stabilization of 80–420 K. The XYZ orthogonal laboratory frame chosen for the EPR line anisotropy pattern is related to the a_h, c_h crystallographic axes [2]: $X \parallel a_h$, $Z \parallel c_h$, $Y \parallel (a_h \times c_h)$.

3. EPR spectra

The EPR spectrum recorded after x-irradiation and repeated a few days later consists of 13 narrow lines with the linewidth $\Delta B_{pp} = 0.25$ mT and line separation $\delta B_0 \approx 0.5$ mT. In the pure x-irradiated $Cs_5H_3(SO_4)_4 \cdot H_2O$ paramagnetic centres are formed in the process $SO_4^{2-} + h\nu \rightarrow SO_4^- + e^-$.

It is expected that the 12 EPR lines should be divided into several structurally nonequivalent SO_4^- paramagnetic units with superhyperfine proton structure due to the electron spin ($S = \frac{1}{2}$) interaction with nearest proton nuclear spins ($I = \frac{1}{2}$).

The EPR spectrum anisotropy in the ZY plane is shown in figure 1. As one can see the lowest-field triplet and highest-field doublets have different extremes.

From the anisotropy data for the XY and ZX planes (not presented here) we have found that the main crystal field z-axis lies in the ZY plane except for the highest-field doublet for which the z crystal field axis is inclined at $\Theta = 25^\circ$ to the ZY plane.

Also the EPR spectrum recorded at two different microwave powers (figure 2) shows different intensity behaviour of the lines consisting of the 13-component spectrum, proving our spectrum division into separate units.

In order to explanation of the EPR spectra observed, we present in figure 3 the projection of the crystal structure [3] of the hexagonal PCTHS phase on the (001) plane. Large open circles represent Cs atoms and the partially filled circles H_2O molecules. The two $SO_4(1)$ and $SO_4(2)$ groups are distinguished. Rotations of the tetrahedra are shown by arrows on the largest circles. The small open circles show the H-bonds perpendicular to the (001) plane. On this picture we have marked in addition the main crystal field z-axes in accord with the extrema (minima) of the EPR spectra in the (001) plane (figure 1).

The essentially different temperature behaviour of the lowest triplet spectrum (marked as ●) and all others presented in the next paragraph allows us to assume that two different $SO_4(1)$ and $SO_4(2)$ units are involved in our complex EPR spectra.

We have marked in figure 3, by the black circles, the possible hydrogen positions near $SO_4(1)$ and $SO_4(2)$ type units after X-irradiation (the black circles replace some of the open circles in the nonirradiated structure), which should give the ‘triplet’ and two lowest ‘doublet’ spectra presented in figure 1.

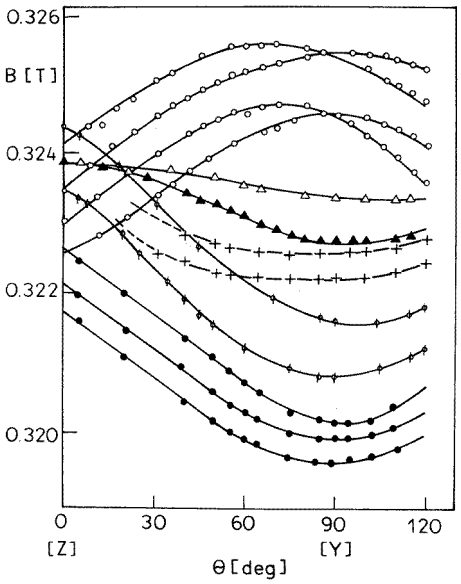

Figure 1. EPR spectra anisotropy in the ZY plane of x-irradiated $Cs_5H_3(SO_4)_4 \cdot H_2O$ at room temperature (RT): ○, H–SO_4^- doublets; ●, H–SO_4^-–H triplet; +, H-SO_4^- doublet; ϕ, H-SO_4^- doublet; Δ, SO_4^- singlet; ▲, free electron, single line.

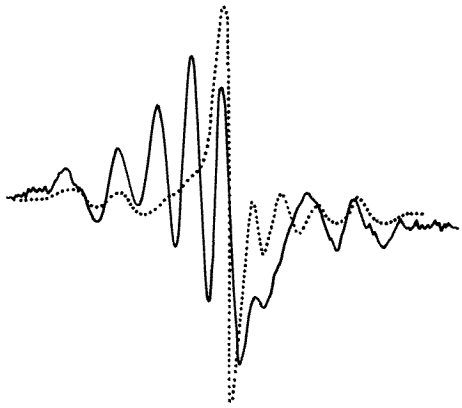

Figure 2. EPR spectra recorded at two different microwave powers: . . ., 20 dB; ——, 6 dB.

Figure 3 with the main z-axes in the XY plane of the complexes under discussion is simplified because simulated anisotropy for 'triplet' spectra needs a small ($\cong 5$) inclination from the XY plane (see figure 4).

A similar structure projection in the ZX plane (not presented here) for the x-irradiated sample should give two high-field doublets of $H(SO_4)^-(1)$ type marked as open circles in figure 1 differently oriented due to $SO_4(1)$ tilting during H-bond formation as claimed by Merinov *et al* [3] and x-irradiation.

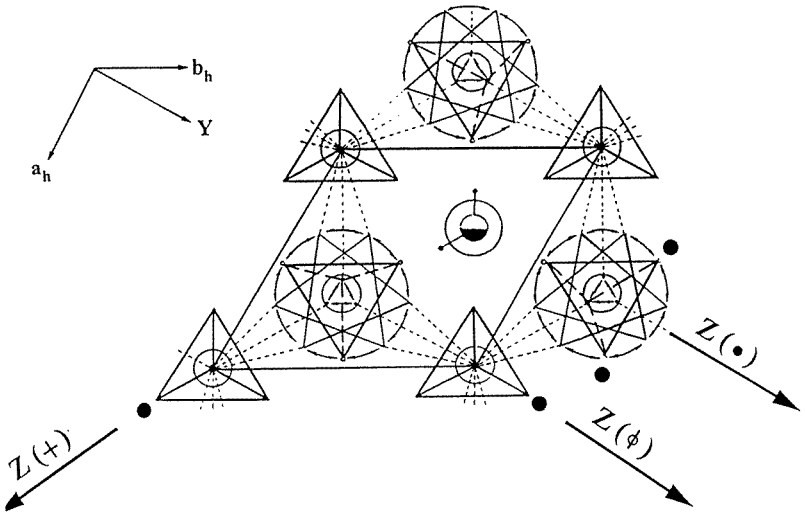

Figure 3. The projection of the crystal structure of hexagonal PCTHS on the (001) plane. Large open circles, Cs atoms; partially filled circle, molecule H_2O. The tetrahedra drawn in the largest circles show the possible reorientations of $SO_4^{2-}(2)$ in contrast to the static $SO_4^{2-}(1)$ tetrahedra connected with $SO_4^{2-}(2)$ by hydrogen bonds marked by dashed lines. Small open circles, H-bonds perpendicular to the (001) plane. In addition we have marked by arrows the main crystal field z-axes for each complex and by black circles the possible proton positions in x-irradiated PCTHS.

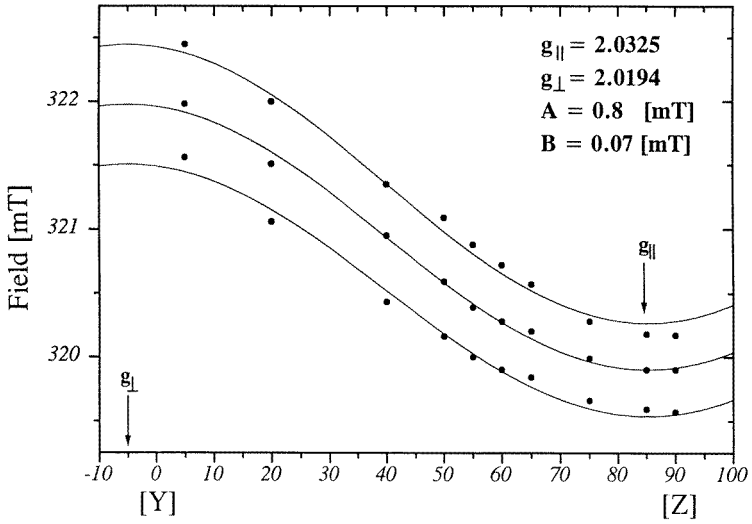

Figure 4. The simulated anisotropy of 'triplet' spectra in the ZY plane of PCTHS. Solid lines, fit; filled circles, experimental data.

Because, as we mentioned above, the superhyperfine proton structure line separation is of the order of the linewidth we cannot neglect the nuclear Zeeman term in the resulting spin Hamiltonian.

In figure 4 we present the anisotropy simulation (solid line) with experimental results (points) for the lowest triplet (figure 1). The simulation has been performed according to the equation of Wertz and Botton [5] for the resonance field:

$$\boldsymbol{B}_r = \boldsymbol{B}_0 \pm \boldsymbol{a}/2 \tag{1}$$

with $\boldsymbol{a} = [A + B(3\cos^2\theta - 1)]h/(g\beta)$, where A is the isotropic part of the superhyperfine proton structure, B is the anisotropic part, and θ is the angle between the z-axis and the external magnetic field $\boldsymbol{B}$.

(1) is fulfilled for $|\boldsymbol{B}_r| \ll |\boldsymbol{B}_{ST}|$ and condition $A \gg B$, where $\boldsymbol{B}_{ST}$ is the magnetic field on the hydrogen nuclei evoked by the electrons.

In this case of $|\boldsymbol{B}_r| \ll |\boldsymbol{B}_{ST}|$ only allowed nuclear transitions should be observed [5]. This is the reason why numbers of superhyperfine EPR lines allow us to 'measure' the number of protons near $SO_4^-(2)$ units.

We presume that condition $|\boldsymbol{B}_r| \ll \boldsymbol{B}_{ST}|$ holds also for the remaining eight lines of $H(SO_4)^-(1)$-type paramagnetic centres. They are distinguished in the ZY plane due to a slight difference of its crystal field axis orientation in space.

In a special orientation the full EPR spectra is covered to the low-field triplet and one doublet with a g_e strong line inside as shown in figure 5.

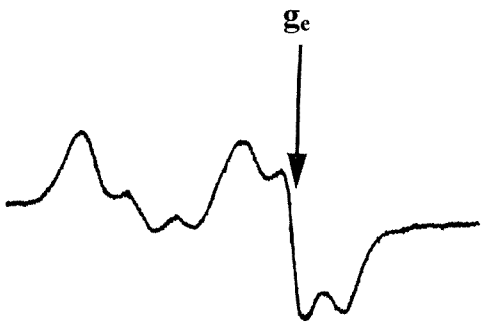

Figure 5. EPR spectra recorded in the ZX plane for $\Theta \cong 5^\circ$ to the Z-axis.

The anisotropy pattern in figure 1 is mainly due to g-factor anisotropies. Than EPR spectra are divided into doublets instead of quartets as expected [5] for $|\boldsymbol{B}_r| \approx |\boldsymbol{B}_{ST}|$.

4. Temperature dependence of the EPR spectra

The temperature dependence of EPR spectra for an external magnetic field directed along $\Theta = 60^\circ$ to $Z(c_n)$-axis (figure 1) and sequences of heating and cooling runs 295 K $\rightarrow$ 95 K $\rightarrow$ 390 K $\rightarrow$ 295 K reveals that only the lowest triplet of H–SO_4(2)–H, with the intensity ratio 1:2:1 at RT, changes due to smooth line broadening. The last nine lines do not change with temperature as demonstrated in figure 6 for a few temperatures.

The smooth EPR line smearing of this lowest superhyperfine triplet is completed at a temperature T_g which depends on the cooling rate and recooling cycles and varies from 203 K for faster cooling to 150 K for slower cooling. Such an EPR spectrum evolution reflects the freezing of rotational dynamics of the SO_4(2) groups.

The SO_4(2) as well as SO_4(1) groups are connected by hydrogen bonds. With temperature lowering the slowing down of acid proton motion in hydrogen bridges is expected.

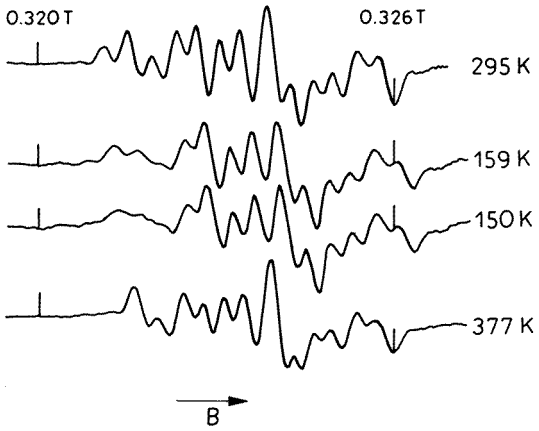

Figure 6. EPR spectrum records for an external magnetic field B along $\Theta = 60^\circ$ to the Z-axis in the ZY plane for a few temperatures: 295, 159, 150 and 377 K.

In KDP-like structures such a slowing down motion leads to EPR line narrowing and splitting [6]. In our case the EPR spectrum of the lowest triplet shows EPR line smearing which means that in addition to slowing down of proton motion the random rotational freezing of $SO_4(2)$ units take place.

For the heating run the lowest-field triplet smoothly changes into a doublet at about 370 K. It should be noted that changes of SO_4 group vibrations near about 370 K have been also detected in Raman spectra [7].

All the above EPR spectra changes versus temperature are reproducible as long as the temperature does not exceed $T \approx 395$ K, where all spectra, except that with $g_e = 2.0023$, disappear due to conversion of SO_4^- paramagnetic centres to nonmagnetic SO_4^{2-}.

The SO_4^- paramagnetic centres are not good probes for studying the fast-proton conductivity above $T \approx 415$ K because they are annealed at higher temperatures. Figure 7 shows this annealing process for a few temperatures. At 415 K all the SO_4^- centres disappear; the line marked as g_e at lower temperature remains very small. A strong line with $g = 2.005$, which may be tentatively described as a line of the SO_2^- radical [8], is recorded, and the sample at this temperature is opaque and 'milk white'.

5. Discussion

$Cs_5H_3(SO_4)_4 \cdot H_2O$ has a structural motif similar to that of $Me_3H(AO_4)_2$ crystals, built up by layers consisting of SO_4 tetrahedra linked by the hydrogen bonds where the acid protons occupy the hydrogen bond position with the probability $\frac{1}{6}$ [1, 9].

Due to superhyperfine electron–proton interaction we can record protonic positions in the ring formed by six SO_4^- tetrahedra.

Figure 8 shows the EPR spectra for six SO_4 tetrahedra linked by hydrogen bonds with the corresponding number of neighbouring protons.

Our 12-EPR-lines spectra are divided into six nonequivalent $HnSO_4^-$ units with $n = 0, 1, 2$ nearest protons in hydrogen bridges.

An unusual behaviour of the lowest triplet with decreasing temperature can be explained as follows: the $SO_4^-(2)$ units, as mentioned above, are orientationally disordered and

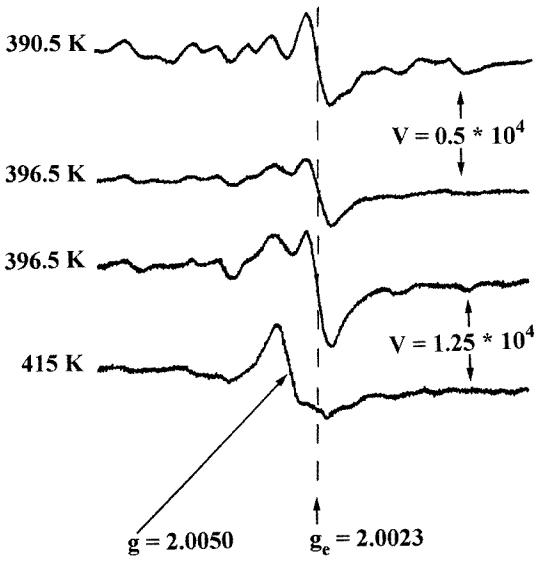

Figure 7. EPR spectrum changes above 390 K.

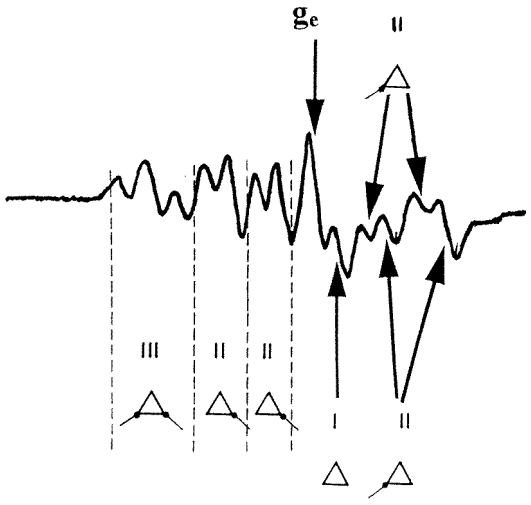

Figure 8. A schematic division of a 12-component EPR spectrum into the $H_nSO_4^-$ configuration; $n = 0, 1, 2$ depending on the number of protons near each of the SO_4^- units.

their site symmetry (C_{3v}) is realized dynamically. Thus two 'close' proton superhyperfine structures of the H–SO_4^-(2)–H paramagnetic centre is realized dynamically as shown in figure 9.

Below RT the superhyperfine structure smearing appears if the SO_4^-(2) motion frequency is lower than the superhyperfine line splitting δH ($\omega_e = \gamma \delta H/\hbar = 1.7 \times 10^7$ s^{-1}).

With increasing temperature, the frequency of SO_4^-(2) motion grows. It follows that the two-'close'-proton superhyperfine structure with intensity ratio 1:2:1 at RT is observed. At about 370 K only one 'close' proton EPR spectrum is recorded which means that the

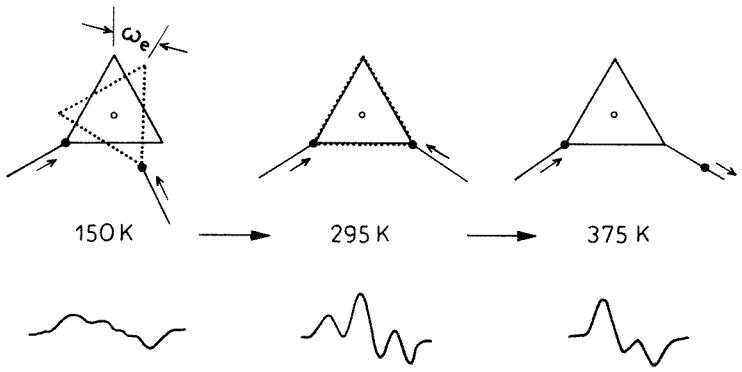

Figure 9. A schematic explanation of the lowest-field EPR spectrum temperature evolution due to dynamical ω_e motion of $SO_4(2)$ type units versus temperature.

second 'close' proton quickly jumps between different H-bond sites (intermolecular proton motion).

Glasslike dielectric dispersion has been detected below $T_g = 260$ K; this is attributed to freezing of the acid hydrogen bond [1] which linked the SO_4 groups into two-dimensional layers.

In addition the proton NMR maximum linewidth occurs around T_g [10], demonstrating the slowing down of acid proton motion and freeze-out of crystalline water reorientations.

Our data, described above, show anomalous behaviour of H–SO_4–H EPR lines which directly indicates the freezing of acid proton dynamics and resulting random rotational freezing of $SO_4^-(2)$ tetrahedra.

The T_g dependence on cooling rate we detect is typical for glasslike systems and reflects peculiarities of the transition between ergodic and nonergodic states.

Another interesting feature in EPR spectra is the reversible transformation of the lowest triplet into a doublet at $T \approx 370$ K. This temperature is close to $T \approx 360$ K where pronounced changes in Raman spectra occur [7].

A model proposed by Yuzyuk *et al* [7, 11] tries to explain these anomalies by the orientational disordering of $SO_4(1)$ type groups occupying 4(e) positions. This means that above about 360 K two $SO_4(1)$ and $SO_4(2)$ groups are energetically equivalent—unlike the case at lower temperatures. Our EPR data are not in conflict with this model.

As can be seen from figure 6, at lower temperatures the full EPR spectra recorded consist of lowest-field triplet and highest-field doublets; above $T \approx 370$ K the lowest-field triplet transforms to a doublet. As a result the spectrum is built from doublets, which means that $SO_4(2)$ and $SO_4(1)$ groups have now the same 'one-proton' configurations.

6. Conclusion

The above results are a direct local proof for the existence of two structurally and dynamically different SO_4 groups in PCTHS at room temperature.

In the temperature range of 200–150 K, depending on cooling rate, only the rotational dynamics of $SO_4(2)$ groups are pronounced. This change of local dynamics is responsible for the glasslike dispersion observed [1]. At about 370 K this specific difference in $SO_4(2)$ and $SO_4(1)$ group dynamics disappears. It is our supposition that this is due to fast interbond

motion. The question of the real number of protons near each SO_4^- unit in the nonirradiated PCTHS crystal is not solved unambiguously anywhere.

In the paper of Kadlec *et al* [12] it is only suggested that during the transition into the glassy phase the rotations of $SO_4^-(2)$ tetrahedra freeze in three different orientations. In this way, nonequivalent $H_3(SO_4)_4^{5-}$ complexes are formed and there are several possibilities for their orientation.

Yuzyuk *et al* [13] claim that hydrogen bonds called 'principals' bind together sulphate groups into isolated complexes $H_3(SO_4)_4^{5-}$ of a 'propeller-like' form, which assume several orientations in the PCTHS structure.

In our case of x-irradiated $Cs_5H_3(SO_4)_4 \cdot H_2O$ where about 10 ppm SO_4^- radicals are produced we may have to deal with a small perturbed zone in the real PCTHS structure. The breaking of the weak part of O–H. . .O bonds leads to H–SO_4 or H–SO_4–H ions [10].

The superhyperfine structure can be seen by the electron located on the sulphur ion only due to S–O–H bonds and only protons 'captured' by SO_4^- unit are seen. The number of protons near SO_4^{2-} units (pure crystals) and SO_4^- (x-irradiated) does not have to be mandatorily the same. Nevertheless different $SO_4^-(2)$ and $SO_4^-(1)$ type tetrahedron dynamics are proved directly by the EPR spectra and 'visualized' for the first time.

The H_2O molecules located between SO_4 layers must be orientationally disordered as well. We cannot look at this problem by the EPR of SO_4^- centres but we observed the H_2O motion freezing indirectly using VO^{2+}, another paramagnetic probe [14].

References

[1] Baranov A I, Kabanov O A, Merinov B V, Shuvalov L A and Dolbinina V V 1992 *Ferroelectrics* **127** 257
[2] Merinov B V, Jones D, Roziere J and Mhiri T 1994 *Solid State Ion.* **69** 53
[3] Merinov B V, Baranov A I, Shuvalov L A, Schneider J and Shulz H 1994 *Solid State Ion.* **74** 53
[4] Courtens E 1987 *Ferroelectrics* **72** 229
[5] Wertz J E and Bolton J R 1972 *Electron Spin Resonance* (New York: McGraw-Hill)
[6] Müller A K 1987 *Ferroelectrics* **72** 273
[7] Yuzyuk Yu I, Dmitriev V P, Loshkarev V V, Rabkin L M and Shuvalov L A 1995 *Ferroelectrics* **167** 53
[8] Atkins P W and Symons M C R 1967 *The Structure of Inorganic Radicals* (Amsterdam: Elsevier)
[9] Merinov B V, Baranov A I, Shuvalov L A and Schagina N M 1991 *Kristallografiya* **36** 584
[10] Fajdiga-Bulat A M, Lahajnar G, Dolinsek J, Slak J, Lozar B, Zalar B, Shuvalov L A and Blinc R 1995 *Solid State Ion.* **77** 101
[11] Yuzyuk Yu I, Dmitriev V P, Rabkin L M, Burmistrova L, Shuvalov L A, Smutny F, Vanek P, Gregora I and Petzelt J 1995 *Solid State Ion.* **77** 122
[12] Kadlec F, Yuzyuk Yu I, Simon P, Pavel P, Łapsa K, Vanek P and Petzelt J 1996 *Ferroelectrics* **176** 179
[13] Yuzyuk Yu I, Dmitriev V P, Rabkin L M, Smutny F, Gregorova I, Dolbinina V V and L A Shuvalov 1996 *J. Phys.: Condens. Matter* **8** 3965
[14] Waplak S *et al* in preparation